

ChemComm

Accepted Manuscript



This is an *Accepted Manuscript*, which has been through the Royal Society of Chemistry peer review process and has been accepted for publication.

Accepted Manuscripts are published online shortly after acceptance, before technical editing, formatting and proof reading. Using this free service, authors can make their results available to the community, in citable form, before we publish the edited article. We will replace this *Accepted Manuscript* with the edited and formatted *Advance Article* as soon as it is available.

You can find more information about *Accepted Manuscripts* in the [Information for Authors](#).

Please note that technical editing may introduce minor changes to the text and/or graphics, which may alter content. The journal's standard [Terms & Conditions](#) and the [Ethical guidelines](#) still apply. In no event shall the Royal Society of Chemistry be held responsible for any errors or omissions in this *Accepted Manuscript* or any consequences arising from the use of any information it contains.

COMMUNICATION

Bisindeno-annulated Pentacenes with Exceptionally High Photo-stability and Ordered Molecular Packing: Simple Synthesis by Regio-selective Scholl Reaction

Cite this: DOI: 10.1039/x0xx00000x

Received 00th January 2014,
Accepted 00th January 2014
DOI: 10.1039/x0xx00000x

Arun Naibi Lakshminarayana,^a Jingjing Chang,^a Jie Luo,^b Bin Zheng,^c Kuo-Wei Huang,^c Chunyan Chi*^a

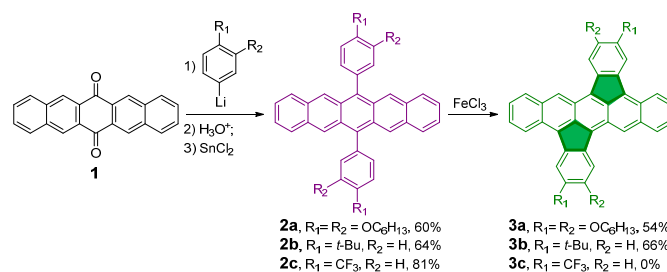
www.rsc.org/

Bisindeno-annulated pentacenes 3a-b were synthesized by a simple regio-selective, FeCl₃-mediated Scholl reaction from the corresponding 6,13-diaryl pentacene precursors. The fusion of two indeno- units dramatically changes the electronic properties and chemical reactivity of pentacene and the obtained compounds exhibited exceptionally high photo-stability in the solution, with a half-life time of 11.2 (3a) and 32.0 (3b) days under ambient light and air conditions. Ordered molecular packing with small π - π stacking distance was observed in the single crystals of 3a and 3b. Our research provides a promising strategy to access stable higher order acenes with controlled molecular order.

Acenes are one of the highly exploited molecules for the organic opto-electronic materials.¹ Poor solubility and low stability of acenes are the prominent issues that limited their application. In recent years, various functionalization strategies have been developed to synthesize relatively stable acene derivatives including high order acenes (i.e., acenes longer than pentacene) up to nonacene.² Nevertheless, these methods could not be extended effectively for the synthesis of acenes longer than nonacene, owing to their readiness to undergo photo-oxidation. So the quest for an alternative approach to obtain more stable high order acenes yet remains. Besides the stability issue, ordered molecular packing with close contacts (e.g., π - π stacking) is essential for their applications in electronic devices such as organic field effect transistors (OFETs), but this requirement usually conflicts with the necessity to introduce bulky substituents to solubilize and kinetically stabilize the highly reactive higher order acenes. This *Communication* demonstrates a new stabilizing strategy and synthetic method to obtain very stable acenes with controlled molecular order by using bisindeno-annulated pentacenes as subjective models.

The fundamental concept of our molecular design is to functionalize acenes with two aryl groups fused on either side along the *peri*-position, such as in the bisindeno-annulated pentacenes **3a-c** (Scheme 1). Previous attempts to stabilize acenes illustrate that appropriate functionalization along the *peri*- positions increases the solubility and imparts varying degree of photo-stability depending on the functionalization moiety and their position. We hypothesized the model to enhance the stability of acenes by fusing an aryl group

onto the *peri*- position such that two sites on the perimeter are kinetically blocked by a single aryl moiety. More importantly, such an annulation results in two cyclopenta- rings which can serve as electron-accepting moieties to stabilize the electron-rich acenes, as already demonstrated in other cyclopenta-fused polycyclic aromatic hydrocarbons (CP-PAHs) such as rubicene³ and cyclopent[hi]aceanthrylene.⁴ Thus, such a strategy is supposed to significantly improve the stability of acenes. The ring fusion would also result in a more rigid core which can facilitate ordered face-to-face molecular stacking in solid state and is desirable for OFET applications. Good solubility can be ensured by introduction of additional alkyl/alkoxy chains onto the aryl moiety. Therefore, our design takes three important criteria into consideration, viz., stability, solubility and molecular packing.



Scheme 1. Synthesis of bisindeno-annulated pentacenes **3a-c**.

The synthetic chemistry of CP-PAHs was recently developed mainly including Pd-catalysed Heck coupling^{3b-e} or pentannulation,^{4a-b} which however are normally limited by low reaction yield. Herein, we demonstrated that the bisindeno-annulated pentacenes **3a-b** can be simply synthesized in considerably good yield by a FeCl₃-mediated Scholl reaction from the easily available 6,13-diaryl pentacene precursors **2a-b** (Scheme 1). FeCl₃-mediated oxidative cyclodehydrogenation (i.e., modified Scholl reaction) has been successfully used for the synthesis of various benzenoid PAHs⁵ and π -extended porphyrins.⁶ Given the electron-rich character of pentacene, we hypothesized that the 6,13-diaryl substituted pentacenes can undergo similar oxidative cyclization reactions to form five-membered rings along the *peri*- position. To test our idea, the 6,13-diaryl pentacenes with electron-donating (3,4-

dihexyloxyphenyl in **2a**, 4-*tert*-butylphenyl in **2b**) or electron-accepting (4-trifluoromethylphenyl in **2c**) aryl substituents were first prepared from pentacenequinone **1** by using standard protocol. To our delight, the FeCl₃ mediated Scholl reaction of **2a/2b** selectively gave the *transoid* double cyclized products **3a/3b** as dark green solid in good yields, while no cyclization was observed with **2c** due to the electron-deficient character of the 4-trifluoromethylphenyl groups. The excellent regio-selectivity likely can be ascribed to the large strain in the *cisoid* isomers. Both the bisindeno-annulated pentacenes **3a/3b** show considerably good solubility in common organic solvents such as dichloromethane, chloroform and toluene and their structures were identified by NMR, mass spectrometry (ESI⁺) and X-ray crystallographic analysis (*vide infra*).

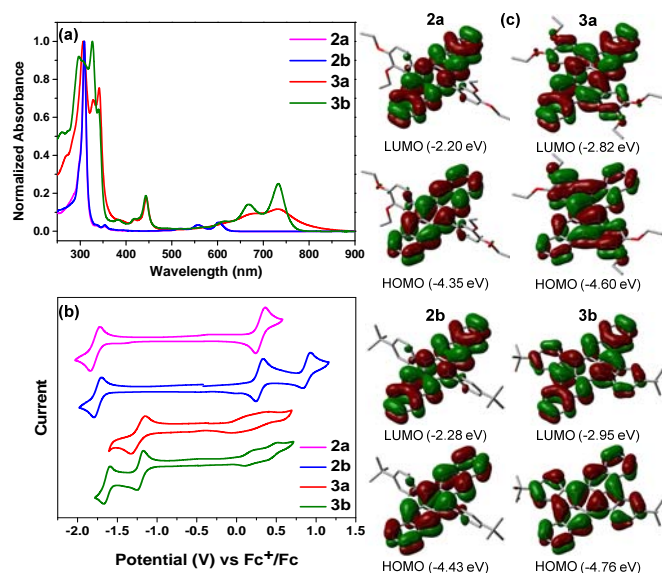


Fig. 1 (a) UV-Vis absorption spectra of **2a-b** and **3a-b** in chloroform; (b) cyclic voltammograms of **2a-b** and **3a-b** in dry dichloromethane; (c) frontier molecular orbital profiles of **2a-b** and **3a-b** based on DFT (B3LYP/6-31G*) calculations.

The 6,13-diaryl substituted pentacenes **2a/2b** showed typical *p*-band absorption with maximum at 603 nm (Fig. 1a), which can be correlated to the HOMO→LUMO transition (oscillator strength $f = 0.1046$ for **2a** and $f = 0.0984$ for **2b**) based on the time dependent density functional theory (TD DFT) calculations (B3LYP/6-31G*) (Table S2-S3 and Fig. S1-S2 in ESI⁺). After ring fusion, the electronic spectra show a large red shift, with an absorption maximum at 732 nm for both, corresponding to HOMO→LUMO transitions ($f = 0.1179$ for **3a** and $f = 0.1785$ for **3b** based on TD DFT) (Table S4-S5 and Fig. S3-S4 in ESI⁺). However, the substantial contribution from the HOMO-1→LUMO transition in case of **3a** results in the spectral broadening. Therefore, the alkyl and alkoxy side chains do not have significant impact on the electronic absorption spectra. The optical energy gap decreased from 1.98 eV for **2b** to 1.63 eV for **3b**. No obvious fluorescence can be observed for both **3a** and **3b**.

Cyclic voltammetry (CV) and differential pulse voltammetry (DPV) measurements show a reversible oxidation wave with half-wave potential $E_{1/2}^{ox}$ at 0.26 V and a reversible reduction wave with half-wave potential $E_{1/2}^{red}$ at -1.80 V (vs. ferrocene/ferrocenium couple, Fc/Fc⁺) for **2a**, whereas **2b** shows two reversible oxidation waves with $E_{1/2}^{ox}$ at 0.26 V and 0.85 V and one reversible reduction wave with $E_{1/2}^{red}$ at -1.75 V (Fig. 1b and Fig. S5 in ESI⁺). A quasi-reversible oxidation wave with $E_{1/2}^{ox}$ at 0.27 V and one reversible reduction wave with $E_{1/2}^{red}$ at -1.24 V were observed for **3a**, while compound **3b** exhibits two quasi-reversible oxidation waves with

$E_{1/2}^{ox}$ at 0.15 and 0.43 V and two reversible reduction waves with $E_{1/2}^{red}$ at -1.22 and -1.65 V. The HOMO/LUMO energy levels were determined to be -5.02/-3.14 eV for **2a**, -5.00/-3.15 eV for **2b**, -4.71/-3.68 eV for **3a** and -4.88/-3.68 eV for **3b** from the onset of the first oxidation/reduction wave.⁷ The corresponding electrochemical energy gaps are then estimated to be 1.88, 1.85, 1.04 and 1.2 eV. DFT calculations indicate that the HOMO and LUMO contours remain along the whole pentacene framework in **2a/2b**. However, after ring fusion, both the HOMO and LUMO are delocalized to the fused bisindeno-units and show somewhat disjoint character (Fig. 2c). Calculations also predicted a significant decrease of HOMO-LUMO energy gaps, which is consistent with the experimental data.

The photo-oxidative decay of **2a/2b** and **3a/3b** were monitored by UV-vis absorption spectroscopy in chloroform solutions (1×10^{-5} M) under same ambient light and air conditions (Fig. 2 and Fig. S6 in ESI⁺). Like many other pentacene derivatives, the pentacene precursors **2a** and **2b** are very reactive and quickly decomposed with a half-life time of 10.5 min and 26 min, respectively. However, the bisindeno-annulated pentacenes **3a/3b** exhibited exceptionally high photo-stability. In both cases, the optical density at 732 nm showed gradual decay with time, with appearance of new band at around 490 nm. The half-life times of 11.2 days (16069 min) and 32.0 days (46031 min) were determined for **3a** and **3b**, respectively, which are even higher than the TIPS-pentacene at similar conditions (1360 min).⁸ The largely enhanced photo-stability of **3a/3b** can be ascribed to the kinetic blocking of the *peri*- positions and formation of electron-accepting cyclopenta- rings.

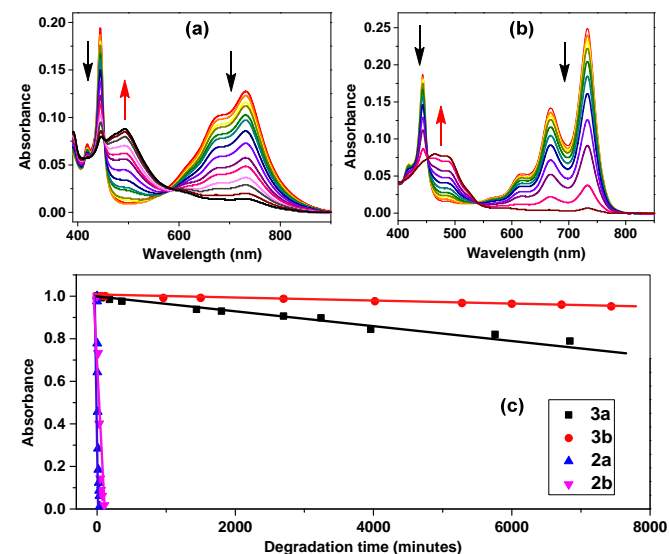


Fig. 2 Changes of the UV-vis absorption spectra of (a) **3a** and (b) **3b** in 10^{-5} M CHCl₃ solutions under ambient light and air conditions. (c) Plots of the optical density at 603 nm (for **2a/2b**) and 732 nm (for **3a/3b**) over the time.

Single crystals of **3a** and **3b** suitable for X-ray crystallographic analysis were obtained by slow diffusion of acetonitrile or methanol into their solutions in chloroform. For both compounds, the bisindeno-annulated pentacene framework has a planar structure and forms columnar superstructure *via* close π -stacking (Fig. 3 and Fig. S7 in ESI⁺). The presence of hexyloxy groups in **3a** leads to a slip face-to-face packing to accommodate the hexyloxy chains in place. Whereas **3b** shows a helical columnar structure and the adjacent pentacene molecules are stacked in anti-parallel motif with a small rotation angle (24.2°) between the pentacene units to keep the bulky *tert*-butyl groups away. Nevertheless, the intermolecular distances of the **3a** and **3b** are appreciably small, i.e., 3.352 Å and 3.359 Å, respectively, which are desirable for charge transport.

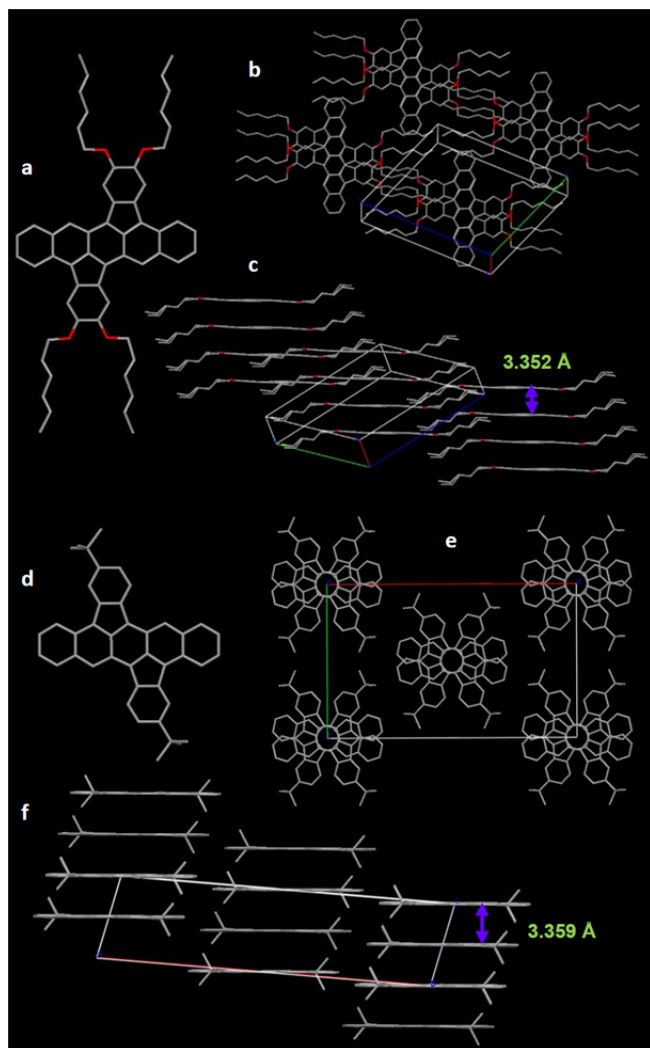


Fig. 3 Crystallographic structures and 3D packing of **3a** (a-c) and **3b** (d-f).

OFETs of **3a** and **3b** were fabricated by solution processed thin films using a bottom-gate top-contact device structure and all devices measured in N_2 exhibited *p*-type behaviour (Fig. S8-S9 in ESI†). An average hole mobility (μ_h) of $0.06 \text{ cm}^2 \text{V}^{-1} \text{s}^{-1}$, threshold voltage (V_T) of -1 V , and current on/off ratio ($I_{\text{on}}/I_{\text{off}}$) of 10^5 were achieved for **3a**. The relatively low performance can be ascribed to the amorphous character and discontinuous micromorphology of the solution-processed thin films as revealed by atomic force microscope and X-ray diffraction measurements, which however were not improved by thermal annealing or modifying the dielectric layer (Table S16 and Fig. S10-12 in ESI†). The devices of **3b** gave worse performance (μ_h : $1.9 \times 10^{-5} \text{ cm}^2 \text{V}^{-1} \text{s}^{-1}$, V_T : -5 V , $I_{\text{on}}/I_{\text{off}}$: 10^3) due to the poor film-forming capability. Further device measurements based on vapour deposited thin films or single crystals will be conducted in the future to exploit the potential of this new type of stable pentacene materials.

In summary, we developed a new strategy to access stable pentacenes by annulation of two indeno- units to the *peri*-position. This was achieved by a simple regio-selective Scholl type cyclization. Our approach resulted in highly stable pentacene derivatives with ordered molecular packing in crystals, which are essential for their practical applications in electronic devices such as

OFETs. Our research provides a general concept to stabilize highly reactive π -conjugated systems such as higher order acenes and periacenes. Currently, these studies are underway in our laboratory.

This work was financially supported from NUS start-up grant (R-143-000-486-133), MOE AcRF grants (R-143-000-510-112 and R-143-000-573-112) and A*STAR JCO grant (1431AFG100). K.-W. Huang acknowledges financial support from KAUST.

Notes and references

^a Department of Chemistry, National University of Singapore, 3 Science Drive 3, 117543, Singapore. Fax: +65 6779 1691; Tel: +65 6516 5375; E-mail: chmcc@nus.edu.sg

^b Institute of Materials Research and Engineering, A*Star, 3 Research Link, Singapore 117602.

^c Division of Physical Sciences and Engineering and KAUST Catalysis Center, King Abdullah University of Science and Technology (KAUST), Thuwal 23955-6900, Kingdom of Saudi Arabia.

† Electronic Supplementary Information (ESI) available: Synthetic procedures and characterization data for all new compounds, DFT calculation details, CV and DPV curves, photo-stability test, OFET fabrication and characterization details, and crystallographic data (CCDC 1035232, 1035233). See DOI: 10.1039/c000000x/

- (a) M. Bendikov, F. Wudl and D. F. Perepichka, *Chem. Rev.*, 2004, **104**, 4891; (b) J. E. Anthony, *Angew. Chem. Int. Ed.*, 2008, **47**, 452. (c) H. Qu, C. Chi, *Curr. Org. Chem.* 2010, **14**, 2070; (d) Q. Ye and C. Chi, *Chem. Mater.*, 2014, **26**, 4046.
- (a) M. M. Payne, S. R. Parkin and J. E. Anthony, *J. Am. Chem. Soc.*, 2005, **127**, 8028; (b) D. Chun, Y. Cheng and F. Wudl, *Angew. Chem. Int. Ed.*, 2008, **47**, 8380; (c) R. Mondal, C. Tonshoff, D. Khon, D. C. Neckers and H. F. Bettinger, *J. Am. Chem. Soc.*, 2009, **131**, 1428; (d) I. Kaur, N. N. Stein, R. P. Kopeski and G. P. Miller, *J. Am. Chem. Soc.*, 2009, **131**, 3424; (e) I. Kaur, M. N. Jazdyk, N. Stein, P. Prusevich and G. P. Miller, *J. Am. Chem. Soc.*, 2010, **132**, 1261; (f) H. Qu and C. Chi, *Org. Lett.*, 2010, **12**, 3360; (g) B. Purushothaman, M. Bruzek, S. R. Parkin, A. F. Miller and J. E. Anthony, *Angew. Chem. Int. Ed.*, 2011, **50**, 7013; (h) H. Qu, W. Cui, J. Li, J. Shao, C. Chi, *Org. Lett.*, 2011, **13**, 924; (i) M. Watanabe, Y. J. Chang, S.-W. Liu, T.-H. Chao, K. Goto, M. M. Islam, C.-H. Yuan, Y.-T. Tao, T. Shinmyozu and T. J. Chow, *Nat. Chem.*, 2012, **4**, 574.
- (a) M. Smet, R. Shukla, L. Fülöp and W. Dehaen, *Eur. J. Org. Chem.*, 1998, 2769; (b) M. Smet, J. Van Dijk and W. Dehaen, *Synlett*, 1999, 495; (c) H. A. Wegner, L. T. Scott and A. de Meijere, *J. Org. Chem.*, 2003, **68**, 883; (d) A. R. Mohebbi, J. Yuen, J. Fan, C. Munoz, M. Wang, R. S. Shirazi, J. Seifter and F. Wudl, *Adv. Mater.*, 2011, **23**, 4644; (e) A. R. Mohebbi and F. Wudl, *Chem. Eur. J.*, 2011, **17**, 2642.
- (a) C. L. Eversloh, Y. Avlasevich, C. Li and K. Müllen, *Chem. Eur. J.*, 2011, **17**, 12756; (b) J. D. Wood, J. L. Jellison, A. D. Finke, L. Wang and K. N. Plunkett, *J. Am. Chem. Soc.*, 2012, **134**, 15783; (c) H. Xia, D. Liu, X. Xu and Q. Miao, *Chem. Commun.*, 2013, **49**, 4301.
- (a) J. Wu, W. Pisula and K. Müllen, *Chem. Rev.*, 2007, **107**, 718; (b) M. Grzybowski, K. Skonieczny, H. Butenschön and D. T. Gryko, *Angew. Chem. Int. Ed.*, 2013, **52**, 9900.
- J. P. Lewtak and D. T. Gryko, *Chem. Commun.*, 2012, **48**, 10069.
- The HOMO and LUMO energy levels were calculated using the following equations: HOMO = $- [E_{\text{ox}}^{\text{onset}} + 4.80]$ eV, LUMO = $- [E_{\text{red}}^{\text{onset}} + 4.80]$ eV, where $E_{\text{ox}}^{\text{onset}}$ and $E_{\text{red}}^{\text{onset}}$ are the onset of the first oxidation and reduction wave (vs. Fc^+/ Fc), respectively.
- L. Abu-Sen, J. J. Morrison, A. B. Horn and S. G. Yeates, *Adv. Opt. Mater.*, 2014, **2**, 636.